Symmetry Breaking of In-Plane Order in Confined Copolymer Mesophases

G. E. Stein,[1] E. W. Cochran,[1,*] K. Katsov,[1] G. H. Fredrickson,[1,†] E. J. Kramer,[1,2,‡] X. Li,[3] and J. Wang[3]

[1]*Department of Chemical Engineering, University of California, Santa Barbara, California, 93106, USA*
[2]*Department of Materials, University of California, Santa Barbara, California, 93106, USA*
[3]*Advanced Photon Source, Argonne National Laboratory, Argonne, Illinois, 60439, USA*

(Received 9 December 2006; published 12 April 2007)

Packing of spherical-domain block copolymer mesophases confined to a thin film is investigated as a function of the number of layers n. We find an abrupt transition from hexagonal to orthorhombic in-plane ordering of domains when n is increased from 4 to 5. As n increases further (up to 23 in this study), the symmetry of the orthorhombic phase asymptotically approaches that of the body-centered cubic (110) plane. These results are interpreted in terms of the energetics of competing packings in the bulk and at the film interfaces. Detailed structural and thermodynamic properties are obtained with self-consistent field theory.

DOI: 10.1103/PhysRevLett.98.158302 PACS numbers: 82.35.Jk, 82.20.Wt, 83.80.Uv

Soft condensed matter can exhibit unusual phases in confinement. For example, confining a colloidal suspension between two walls produces a series of entropy-driven transitions between in-plane hexagonal and square lattices with increasing wall separation [1–4]. Freestanding films of thermotropic liquid crystals also demonstrate a rich variety of thickness-dependent phase behavior, where the crossover from 2D to 3D is not a single first-order phase transition, but is observed to be a series of dislocation-mediated restacking transitions [5–7]. While both colloids and liquid crystals have long been used as models for low-dimensional behavior, the spherical domain morphology observed in highly asymmetric block copolymers is a particularly interesting model system. In a monolayer film, the spherical block copolymer domains arrange on a hexagonal (hex) lattice, while the bulk equilibrium morphology is body-centered cubic (bcc). These symmetries minimize packing frustration in 2D and 3D, respectively [8–10]. However, the nature of the transition from a 2D close-packed structure to a 3D lattice with no close-packed planes is unclear. It has been suggested that multilayer films adopt the bcc lattice with the closest-packed (110) plane oriented parallel to the substrate [11,12]. This orientation minimizes the amount of chain stretching required to fill interstitial space at the substrate and free interfaces. The symmetry of the bcc (110) plane closely resembles that of the hexagonal lattice, so we might expect to see changes in the symmetry of this plane mediate the transition from hex to bcc.

Poly(styrene-*b*-2-vinyl pyridine) (PS-PVP) diblock copolymer was synthesized by anionic polymerization. The polydispersity index is 1.04, the overall degree of polymerization is $N = 626$, and the composition is 12% PVP by volume. The PVP minority component forms spherical domains in a PS matrix. The Flory interaction parameter for PS-PVP is $\chi = 63/T - 0.033$ [13]. The bulk order-disorder transition occurs at $250 \pm 7\,^{\circ}\mathrm{C}$ ($\chi N \approx 54$). Films of PS-PVP ranging from 1–23 layers thick were prepared by spin casting from dilute toluene solutions onto 5 mm thick, 2 in. diameter silicon substrates. The film thickness was controlled by solution concentration (1–5 wt. %) and spin rate (2000–4500 RPM). Samples are thermally annealed under high vacuum (10^{-7} Torr) according to two thermal profiles: (1) A short anneal above the order-disorder transition at $270 \pm 5\,^{\circ}\mathrm{C}$, followed by cooling to $215 \pm 5\,^{\circ}\mathrm{C}$ ($\chi N \approx 60$) and isothermal annealing for 3 days; and (2) a short heating period from room temperature to $215 \pm 5\,^{\circ}\mathrm{C}$ followed by a 3 day isothermal anneal. The PVP block strongly wets the substrate and forms a brush layer. The layers of spherical domains form on top of the brush. When the as-cast film thickness is incommensurate with the equilibrium layer thickness, island or hole structures form at the free surface to relieve frustration and recover the equilibrium layer periodicity.

The lattice symmetry was measured with grazing-incidence small-angle x-ray scattering. These experiments were conducted on the sector 1 and 8 beam lines at the Advanced Photon Source of Argonne National Laboratory, operating at energies of 11.8 and 7.4 keV, respectively. The incident beam illuminates the sample at an angle $\alpha_i \sim 0.1°$, and the diffracted intensity is recorded with a 2D detector. The resulting data set is a map of scattered intensity $I(2\Theta, \alpha_f)$, where 2Θ and α_f denote the in-plane and out-of-plane diffraction angles. In the small-angle approximation, the in-plane scattering vector is $q_{par} \approx 4\pi\Theta/\lambda$. For these experiments, α_i was varied about the critical angle of the polymer $\alpha_{C,P}$ over $0.6 \leq \alpha_i/\alpha_{C,P} < 1.2$ to produce controlled penetration depths ranging from approximately 10 nm up to the full film thickness. This enables us to determine whether the structure is uniform throughout the depth of the film. The incident angle is always less than the critical angle of silicon ($\alpha_{C,Si} \approx 1.5\alpha_{C,P}$), so transmission through the substrate is prevented. The combined effects of reflection from the polymer-substrate interface and diffraction from the internal film structure complicate the out-of-plane analysis

[14,15], so for the purposes of this Letter, we restrict discussion to the in-plane symmetry.

Background corrected profiles of scattering intensity along q_{par} are shown in Fig. 1. The change in symmetry with increasing film thickness (number of sphere layers n) is evident. The symmetry in films 1–3 layers thick is consistent with the hexagonal lattice, with the first three reciprocal space peak positions in the ratio of $q^\star$:$\sqrt{3}q^\star$:$2q^\star$ [the ratio of peak positions for the bcc (110) plane is $q^\star$:$\sqrt{4/3}q^\star$:$\sqrt{8/3}q^\star$]. However, the symmetry in films thicker than 3 layers does not match either the hexagonal lattice or the bcc (110) plane. We therefore propose a general 2D model to fit the data, using the symmetry of the bcc (110) plane to provide an initial estimate of the model parameters.

A 2D lattice can be described completely by two vectors, which we define as $\mathbf{a}_1 = (a_1 \sin\phi, a_1 \cos\phi)$ and $\mathbf{a}_2 = (0, a_2)$, illustrated by Fig. 2(a). The experimental peak positions are fit to the model using a_1, a_2, and ϕ as adjustable parameters. These results are presented in Fig. 2(b), where the symmetry is characterized by the ratio of the second-to-first nearest neighbor distance a_1/a_2, and the lattice angle ϕ. Hexagonal symmetry ($a_1/a_2 = 1$, $\phi = 60°$) is observed for films 1–3 layers thick. At $n = 4$, coexistence between the hex symmetry and an orthorhombic (fco) phase with $a_1/a_2 \approx 1.08$, $\phi \approx 57°$ is observed, where the hex phase is the majority. As n is further increased from 4, a single ort phase is observed, where a_1/a_2 increases asymptotically to a value of 1.17, and ϕ decreases monotonically to 54.2°. From measurements below (open symbols) and above (closed symbols) the critical angle of the polymer, we determine that all structures are uniform throughout the depth of the film. We note that with the exception of $n = 4$, the observed symmetry is independent of the annealing profile, indicating that these are equilibrium phases. The coexistence observed at $n = 4$ suggests that the free energies of the hex and fco phase are nearly degenerate, but after a week of annealing the ort phase is not detected, which suggests that the hex symmetry is stable.

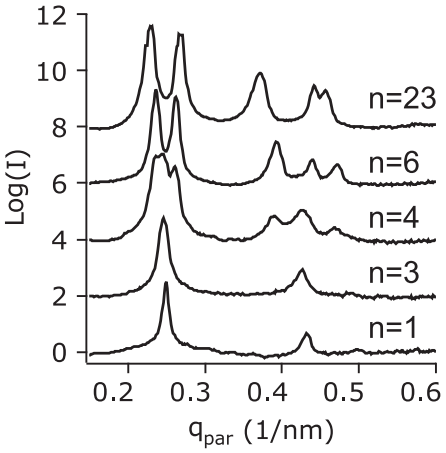

FIG. 1. Intensity line profiles of data collected at $\alpha_i \approx 1.05\alpha_{C,P}$ for films having different numbers of layers n.

To interpret these results we use self-consistent field theory (SCFT) to study structural and energetic properties of block copolymer films confined between two walls. A full SCFT treatment of this problem, while possible, would require expensive large-scale computations for the multilayer films. Instead, we use physical arguments to develop a semiphenomenological framework derived from SCFT calculations for relatively small systems.

To describe the morphological transition, we define the order parameter $\eta \equiv a_1/a_2$, which is a monotonic function of the number of layers n. Following standard treatments of interfacial phenomena, we split the free energy of the n-layer system as

$$F_n(\eta) = F_n^b(\eta) + \Delta F_n^s(\eta), \tag{1}$$

where the first term is the free energy of an n-layer reference bulk system and the second term is an interfacial excess free energy due to the presence of the film surfaces.

The range of interactions between the polymer segments and the wall surfaces is small when compared to the film thickness, which allows us to assume that the interfacial excess quantities are independent of n. For the thickness of an equilibrium multilayer film this results in the following equality $d_n(\eta) - nd_1^b(\eta) = d_1(\eta) - d_1^b(\eta)$, and allows us to express the thickness of an n-layer film in terms of the 1-layer film and bulk layer thicknesses:

$$d_n(\eta) = d_1(\eta) + (n-1)d_1^b(\eta). \tag{2}$$

Similarly, the free energy of the n-layer film can be obtained from $F_n(\eta) - F_n^b(\eta) = F_1(\eta) - F_1^b(\eta)$, which gives the free energy per chain in the n-layer film in terms of that of the 1-layer film and the bulk:

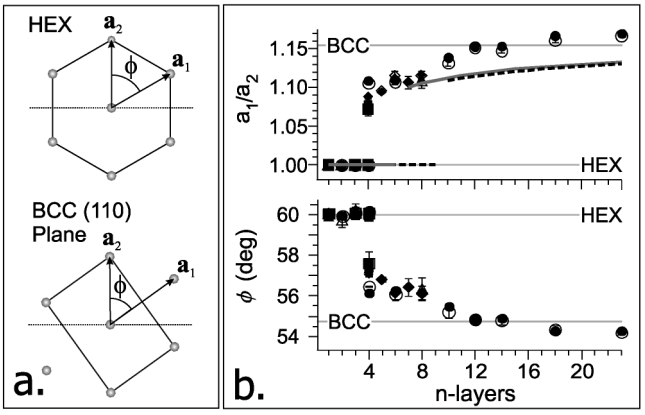

FIG. 2. (a) Illustration of the model parameters for the hex lattice and the bcc (110) plane. (b) Ratio of second-to-first nearest neighbor spacing $a_1/a_2 = \eta$ and lattice angle ϕ as a function of the number of layers n. Error bars encompass ± 1 standard deviation. Lines are SCFT predictions for $\chi N = 50$ (dashed) and 60 (solid).

$$f_n(\eta) = f^b(\eta) + \frac{d_1(\eta)}{d_n(\eta)}[f_1(\eta) - f^b(\eta)]. \quad (3)$$

Qualitative properties of the free energy functions can be analyzed based purely on symmetry considerations. The free energy of a single-layer film $f_1(\eta)$ has to be extremal for the highly symmetric hexagonal domain packing ($\eta^{\mathrm{hcp}} = 1$). Moreover, since η^{hcp} describes the optimal packing of domains in 2D it also corresponds to a global minimum of $f_1(\eta)$. The bulk free energy $f^b(\eta)$ has a more complicated structure. According to Burgers's picture of martensitic transformations [16], the bcc and hcp packings can be continuously deformed into each other. The deformation involves compression along $[100]_{\mathrm{bcc}}$ and elongation along $[110]_{\mathrm{bcc}}$ with a subsequent translation of every other $(110)_{\mathrm{bcc}}$ plane (the so-called "shuffle"). This transformation maps $(110)_{\mathrm{bcc}}$ planes to $(0001)_{\mathrm{hcp}}$ planes while maintaining them parallel to the film surface. The compression and elongation are described by the order parameter η in the range between $\eta^{\mathrm{hcp}} = 1$ and $\eta^{\mathrm{bcc}} = 2/\sqrt{3}$, whereas the shuffle amplitude is relaxed by optimization in the SCFT framework. The high (cubic) symmetry of the bulk bcc phase produces an *additional* minimum in the free energy of the bulk system $f^b(\eta)$ at $\eta^{\mathrm{bcc}} = 2/\sqrt{3}$ [17].

It is clear that the film confinement can destabilize the bulk bcc phase in favor of the hex intralayer packing and therefore *continuously* deform the bcc packing into the face-centered orthorhombic (fco) lattice. Moreover, sufficiently strong surface preference for hex can destabilize the fco packing and result in a *first-order* transition to the hex-packed structure.

To evaluate $f_n(\eta)$ according to Eqs. (2) and (3), we use numerical SCFT [18] to compute the bulk and single-layer quantities d_1, d_1^b, f_1, and f^b. Additionally, we calculated $f_2(\eta)$ at $\chi N = 50$ for a 2-layer film to verify the approximate form in Eq. (3). Since there are many excellent detailed treatments of SCFT available [17,19,20], here we address only the most salient features of the calculations. To impose the thin film confinement, we employ a masking technique described in a recent paper [21] and similar to that used in a thin film study by Matsen [22]. The SCFT equations were solved using algorithms described elsewhere [23,24]. For bulk calculations, the dimensions of the unit cell were continuously adjusted to minimize the microscopic stress [25] in 3D subject to the constraint of fixed η. For $f_1(\eta)$ calculations, the stress was minimized in the plane of the film, while the film thickness $d_1(\eta)$ was adjusted to minimize $f_1(\eta)$. We also adjusted the strength of wall interactions so that the 1-layer film is tensionless relative to the bulk bcc phase. This corresponds to the experimental conditions under which stable supported thin films wet the substrate.

To study potential trends in phase behavior we solved the SCFT equations for three different degrees of segregation: $\chi N = 41$ (nearly disordered) and $\chi N = 50$ and 60 (intermediately segregated). The calculation results for the three cases are summarized in Fig. 3. The qualitative features of the free energy curves are in agreement with the symmetry based predictions.

The general "mechanism" of the transition is shown in Fig. 4. Clearly, as the number of layers in a film increases, the free energy $f_n(\eta)$ develops an additional local minimum at $\eta > 1$. This minimum becomes a global one for sufficiently thick films and the system undergoes a discontinuous transition from hex to fco packing. Figure 4 also shows points at which we calculated $f_2(\eta)$ directly without use of Eq. (3). Near $\eta = 1$ the approximate form of f_2 is nearly exact, whereas for larger values of η Eq. (3) slightly overestimates the surface contribution. The optimal order parameter $\eta(n)$ is shown in Fig. 2(b) for $\chi N = 60$ (solid lines) and $\chi N = 50$ (dashed lines). At $\chi N = 41$ the transition is predicted for $n = 119$ layers and is off the figure scale.

Our calculations also show that the layer thicknesses $d_1(\eta)$ and $d_1^b(\eta)$ are only weakly dependent on η, consistent with experimental results [15]. Under the approximation that $d_1^b(\eta) = d_1(\eta) = \text{const.}$ we can derive a simple estimate for the critical number of layers at the transition

$$n^* \approx 1 + \frac{f_1(\eta^{\mathrm{bcc}}) - f_1(\eta^{\mathrm{hcp}})}{f^b(\eta^{\mathrm{hcp}}) - f^b(\eta^{\mathrm{bcc}})}, \quad (4)$$

which makes the competition between the bulk and surface thermodynamics very transparent. According to Eq. (4), $n^* \approx 9$, 12, 119 for $\chi N = 60$, 50, 41, correspondingly, which can be compared with $n^* = 7$, 10, 119 as predicted by the full theory.

The SCFT calculations at $\chi N = 60$ roughly correspond to the experimental conditions and provide a semiquantitative description of the experimentally observed dependence of η on n. The reason that the theory predicts a relatively large value of $n^* = 7$, when compared to the experimental result $n^* = 5$, can be attributed to a slightly

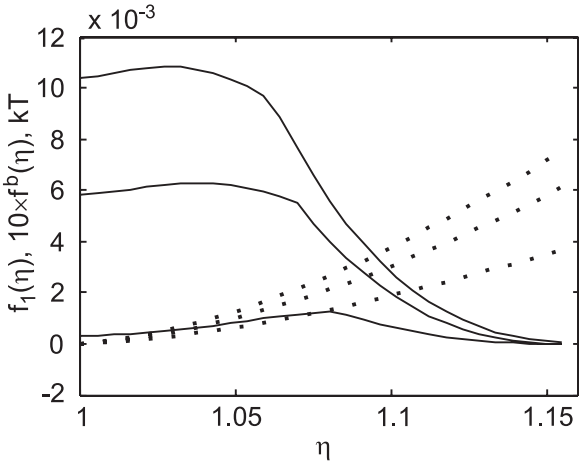

FIG. 3. SCFT free energy per molecule versus the order parameter η from bulk (solid lines) and 1-layer film (dotted lines) calculations. Segregation strength $\chi N = 60$, 50, 41, from top to bottom.

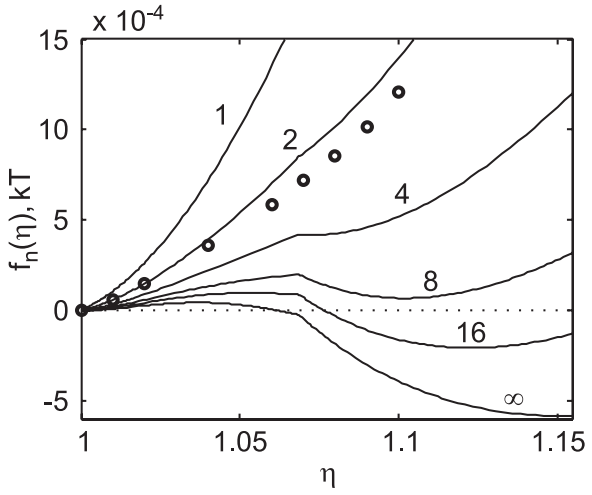

FIG. 4. Free energy variation of multilayer films versus order parameter η at $\chi N = 50$ for films with different numbers of layers. Curves: calculated from Eq. (3). Symbols: computed directly with SCFT for $n = 2$.

different type of confinement used in our calculations and the experiment. In the experiments, the PVP block wets the silicon substrate, so the layers of spheres are formed on top of a PS brush. In our calculations, both film surfaces are modeled with a fixed profile masking technique that results in overestimation of entropic confinement costs and film tension $f_1(\eta)$, which enters the numerator of Eq. (4).

We also note that above the transition ($n > n^*$) the free energy functions in Fig. 3 can be accurately approximated by parabolas:

$$f^b(\eta) \approx \frac{\kappa^b}{2}(\eta - \eta^{\mathrm{bcc}})^2 \quad \text{and} \quad f_1(\eta) \approx \frac{\kappa_1}{2}(\eta - \eta^{\mathrm{hcp}})^2,$$

where κ_1 and κ^b are elastic constants of hex and bcc (110) films. In combination with Eqs. (2) and (3), this Landau-like free energy expansion leads to the following order parameter dependence:

$$\eta(n) = \eta^{\mathrm{bcc}} + \frac{\eta^{\mathrm{hcp}} - \eta^{\mathrm{bcc}}}{1 + (n-1)\frac{\kappa^b}{\kappa_1}}, \qquad n > n^*, \qquad (5)$$

which is indistinguishable numerically from the full numerical solution shown in Fig. 2.

In summary, we find a complex transition from 2D to 3D packing in thin films of spherical-domain block copolymers as a function of film thickness. The 2D hexagonal symmetry is preserved through $n = 4$ layers. At $n = 5$, the hexagonal symmetry breaks to form an orthorhombic phase with in-plane symmetry intermediate between the hcp phase and the bcc (110) plane. As n is further increased from 5 to 23, the orthorhombic unit cell deforms continuously and approaches a value close to the bcc (110) plane. SCFT calculations provide a semiquantitative description of the transition and confirm that it is a consequence of competition between the optimal hex packing at the film surfaces with the preferred $(110)_{\mathrm{bcc}}$ intralayer packing in the bulk.

We appreciate financial support from NSF DMR Polymers and CMMT Programs Contracts No. DMR0307233 and No. DMR0603710. Use of the APS was supported by the U.S. DOE, Office of Science, Office of Basic Energy Sciences, under Contract No. DE-AC02-06CH11357. This work was partially supported by the MRSEC Program of the National Science Foundation under Contract No. DMR05-20415. We thank R. A. Segalman for synthesis of the PS-PVP diblock copolymer used in these studies.

*Current address: Department of Chemical Engineering, Iowa State University, Ames, Iowa 50011-2230, USA.
†Electronic address: ghf@mrl.ucsb.edu
‡Electronic address: edkramer@mrl.ucsb.edu

[1] P. Pieranski, L. Strzelecki, and B. Pansu, Phys. Rev. Lett. **50**, 900 (1983).
[2] D. H. Vanwinkle and C. A. Murray, Phys. Rev. A **34**, 562 (1986).
[3] M. Schmidt and H. Lowen, Phys. Rev. Lett. **76**, 4552 (1996).
[4] C. Ghatak and K. G. Ayappa, Phys. Rev. E **64**, 051507 (2001).
[5] J. Collett *et al.*, Phys. Rev. Lett. **52**, 356 (1984).
[6] J. Collett *et al.*, Phys. Rev. A **32**, 1036 (1985).
[7] J. P. Hirth *et al.*, Phys. Rev. Lett. **53**, 473 (1984).
[8] E. L. Thomas *et al.*, Macromolecules **20**, 2934 (1987).
[9] E. L. Thomas *et al.*, Nature (London) **334**, 598 (1988).
[10] M. W. Matsen, J. Phys. Condens. Matter **14**, R21 (2002).
[11] H. Yokoyama *et al.*, Macromolecules **31**, 8826 (1998).
[12] H. Yokoyama, T. E. Mates, and E. J. Kramer, Macromolecules **33**, 1888 (2000).
[13] K. H. Dai and E. J. Kramer, Polymer **35**, 157 (1994).
[14] B. Lee *et al.*, Macromolecules **38**, 4311 (2005).
[15] G. E. Stein *et al.*, Macromolecules **40**, 2453 (2007).
[16] W. G. Burgers, Physica (Amsterdam) **1**, 561 (1934).
[17] M. W. Matsen and M. Schick, Phys. Rev. Lett. **72**, 2660 (1994).
[18] E. Helfand and Y. Tagami, J. Chem. Phys. **56**, 3592 (1972).
[19] M. W. Matsen, J. Phys. Condens. Matter **14**, R21 (2002).
[20] G. H. Fredrickson, *The Equilibrium Theory of Inhomogeneous Polymers* (Oxford University, Oxford, 2006).
[21] V. Khanna *et al.*, Macromolecules **39**, 9346 (2006).
[22] M. W. Matsen, J. Chem. Phys. **106**, 7781 (1997).
[23] H. D. Ceniceros and G. H. Fredrickson, Multiscale Model. Simul. **2**, 452 (2004).
[24] E. W. Cochran, C. J. Garcia-Cervera, and G. H. Fredrickson, Macromolecules **39**, 2449 (2006); **39**, 4264 (2006).
[25] J.-L. Barrat, G. H. Fredrickson, and S. W. Sides, J. Phys. Chem. B **109**, 6694 (2005).